

# Search for new physics with rare charm decays at LHCb

A. Scarabotto

LPNHE, Sorbonne Université, CNRS/IN2P3, Paris, France.

Received 23 December 2021; accepted 23 February 2022

The LHCb experiment is playing a crucial role in the study of rare and forbidden decays of charm hadrons, which are unique probes for hints of physics beyond the Standard Model. These proceedings present results of the search for semileptonic three-body decays of the form  $D_{(s)}^+ \rightarrow h^\pm \ell^+ \ell'^{\mp}$ , where  $h^\pm$  is a charged pion or kaon and  $\ell'^{\mp}$  is an electron or a muon. Furthermore, studies of the four-body neutral meson charm decays  $D^0 \rightarrow \pi^+ \pi^- \mu^+ \mu^-$  and  $D^0 \rightarrow K^+ K^- \mu^+ \mu^-$  are discussed. Prospects for leptonic and semileptonic rare charm decays at LHCb in the future are presented in the end.

**Keywords:** Rare charm decays; new physics; flavour changing neutral currents.

DOI: <https://doi.org/10.31349/SuplRevMexFis.3.0308053>

## 1. Introduction

The study of rare charm decays constitutes an important test of the Standard Model (SM) and provides a unique window to look for new physics (NP). Searches for rare and forbidden charm decays include a variety of physics processes, ranging from radiative decays with branching fractions (BFs)  $\mathcal{O}(10^{-4})$  to those that are strictly forbidden in the SM, such as decays that violate the conservation of lepton flavour (LFV) and lepton number (LNV).

Leptonic and semileptonic rare charm decays are sensitive to flavour-changing neutral current (FCNC)  $c \rightarrow u\ell\ell$  transitions and constitute complementary studies to down-type quark FCNCs in the kaon and  $b$ -physics sectors. These FCNC processes occur only at loop level in the SM and are highly suppressed by the Glashow-Iliopoulos-Maiani (GIM) mechanism [1]. The BF of  $D \rightarrow X\ell^+\ell^-$  decays, where  $X$  is one or several additional hadrons, is expected to be  $< 10^{-9}$  [2]. However, the BFs can increase up to  $\mathcal{O}(10^{-6})$  as in charm, such decays are dominated by tree-level processes involving intermediate resonances that subsequently decay into two leptons. Precise theoretical predictions of BFs for these resonant modes are difficult to compute, as these processes are dominated by QCD effects at low energies which are evaluated with non-perturbative methods. However, some NP models predict large enhancements of the BFs in regions of the decay phase space away from resonances, and sizeable  $CP$  and angular asymmetries in their vicinity [2–7].

The huge charm production cross section at the Large Hadron Collider, with approximately  $10^{13}$   $c\bar{c}$  pairs produced with the Run1 and Run2 data, allowed the LHCb Collaboration to perform many studies on rare charm decays. The LHCb detector [8, 9] is a single arm forward spectrometer comprising excellent tracking, vertexing and particle identification (PID) optimized for flavour physics studies. A selection of analyses performed by LHCb is presented in this document, focusing on charm mesons decays with three or four charged tracks in the final state.

First, in Sec. 2 the search for decays in the form  $D^+ \rightarrow h^\pm \ell^+ \ell'^{\mp}$  and  $D_{(s)}^+ \rightarrow h^\pm \ell^+ \ell'^{\mp}$ , where  $h^\pm$  is a charged pion or kaon and  $\ell'^{\mp}$  is an electron or a muon, is presented. Sections 3 and 4 show results on the four body decays  $D^0 \rightarrow h^+ h^- \mu^+ \mu^-$  where  $h$  is a pion or a kaon. The analysis reaching the first observation of these decays is presented, followed by a first measurements of interesting asymmetries.

## 2. Search for $D_{(s)}^+ \rightarrow h^\pm \ell^+ \ell'^{\mp}$

The search for 25 decays of type  $D_{(s)}^+ \rightarrow h^\pm \ell^+ \ell'^{\mp}$  is performed on a data sample corresponding to an integrated luminosity of  $1.6 \text{ fb}^{-1}$  collected by the LHCb experiment during part of Run2 [10]. The physics processes of these channels vary, involving:

- rare FCNC transitions of type  $D_{(s)}^+ \rightarrow h^+ \ell^+ \ell^-$ ,
- LFV decays with two oppositely charged leptons of different flavour, *i.e.*  $D_{(s)}^+ \rightarrow h^+ \ell^+ \ell'^-$ ,
- modes with leptons with same electrical charge (with same and different flavour) which are both LFV and LNV of type  $D_{(s)}^+ \rightarrow h^- \ell^+ \ell'^+$ .

Among this list, the SM allowed decays can proceed at tree-level via intermediate resonances ( $\eta, \rho, \omega$  and  $\phi$ ). These are vetoed removing the dilepton mass region [ $525 \text{ MeV}/c^2, 1250 \text{ MeV}/c^2$ ]. The four resonant decays ( $D_{(s)}^+ \rightarrow (\phi \rightarrow \mu^+ \mu^-) \pi^+$ ,  $D_{(s)}^+ \rightarrow (\phi \rightarrow e^+ e^-) \pi^+$ ) are used for calibration and normalisation.

Signal decays are selected requiring three tracks, to form a  $D_{(s)}^+$  secondary vertex with a good fit quality and to satisfy PID and momentum requirements. The  $D_{(s)}^+$  candidate is required to be compatible with a reconstructed primary vertex.

Backgrounds can originate from random combinations of tracks (combinatorial) and fully hadronic three-body misidentified decays. A multivariate (MV) classifier is trained and tested specifically to distinguish signal from combinatorial background, using as input kinematics and topological

variables. Furthermore, PID selections are applied to suppress mis-identified backgrounds which can have a branching fraction up to seven orders of magnitude larger than the signal. After the full selection, the signal yields are determined through a maximum-likelihood fit to the invariant mass distributions in each of the  $D_{(s)}^+ \rightarrow h^\pm \ell^+ \ell'^{\mp}$  decays, including the normalisation modes. The signal and background models used to describe the data are obtained from simulated events.

Electrons lose momentum due to bremsstrahlung radiation when interacting with the detector's material. This degrades the  $D_{(s)}^+$  mass resolution, producing a long tail of events on the left-hand of the known mass of the  $D_{(s)}$  mesons [11]. A procedure to recover the energy loss of bremsstrahlung photons is in place at LHCb. This looks for energy deposits in the electromagnetic calorimeter in the cone around the electron track and adds them back to the electron(s) invariant mass. To model the signal distributions for final states with electrons, separate shapes are extracted from simulation for candidates with and without associated bremsstrahlung photons, which are then combined into a single overall shape according to their relative abundances in simulation.

The branching fraction measurements are performed relative to the already mentioned normalisation channels. This method allows to largely cancel many effects of uncertainties coming from the charm production cross section and detector-induced effects, therefore reducing many systematic uncertainties.

No significant signal is observed in any of the 25 decay channels and an upper limit on the signal BFs using the  $CL_s$  method is set [12]. Upper limits at 90 % confidence level on the branching fractions are found between  $1.4 \times 10^{-8}$  and

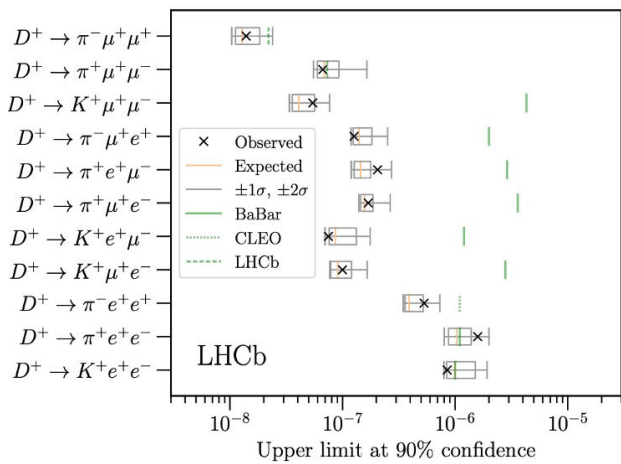


FIGURE 1. Upper limits at 90% confidence level on the  $D^+$  signal channels. The observed limit is given by a black cross, with  $\pm 1\sigma$  and  $\pm 2\sigma$  limits shown as box plots and the median in orange. The green lines show the previous world's best limit from BaBar, CLEO and LHCb [13–15].

$6.4 \times 10^{-6}$  (see Fig. 1). These results improve upon prior world's best constraints by up to a factor of 500.

### 3. Observation of $D^0 \rightarrow h^+ h^- \mu^+ \mu^-$ decays

The semileptonic rare charm decays  $D^0 \rightarrow \pi^+ \pi^- \mu^+ \mu^-$  and  $D^0 \rightarrow K^+ K^- \mu^+ \mu^-$  are observed for the first time by LHCb using a sample of proton-proton collisions corresponding to an integrated luminosity of  $2 \text{ fb}^{-1}$  [16]. The branching fraction measurement is performed in regions of dimuon mass and integrated over the full dimuon-mass range using the SM-dominated decay  $D^0 \rightarrow K^- \pi^+ (\rho^0/\omega \rightarrow \mu^+ \mu^-)$  as a normalisation channel, where the two muons are consistent with originating from intermediate  $\rho^0$  or  $\omega$  resonances. Dimuon-mass regions of the signal modes are defined according the expected intermediates resonances: (low mass)  $< 525 \text{ MeV}/c^2$ , ( $\eta$ )  $525\text{-}565 \text{ MeV}/c^2$ , ( $\rho^0/\omega$ )  $565\text{-}950 \text{ MeV}/c^2$ , ( $\phi$ )  $950\text{-}1100 \text{ MeV}/c^2$ , (high mass)  $> 1100 \text{ MeV}/c^2$ , where for  $D^0 \rightarrow K^+ K^- \mu^+ \mu^-$  decays the limited phase space restricts the measurement to the first three regions.

$D^0$  mesons are required to originate from the decay chain  $D^{*+} \rightarrow D^0 \pi^+$ . This allows to efficiently suppress combinatorial background by selecting a narrow window of  $2 \text{ MeV}/c^2$  in the mass difference  $\Delta m = m(D^{*+}) - m(D^0)$  around its known maximum [11]. Further combinatorial background suppression is achieved by a MV classifier. Peaking background arises from  $D^0 \rightarrow h^+ h^- \pi^+ \pi^-$  decays, where two pions are mis-identified as muons, which have large branch-

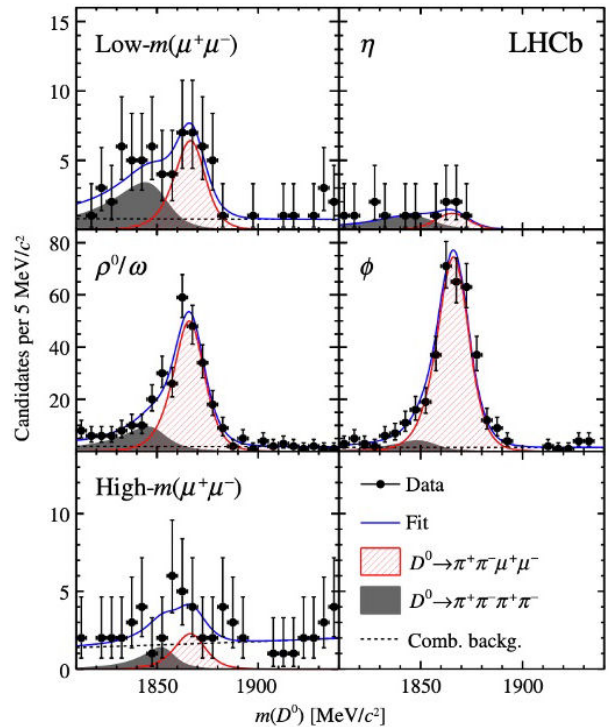


FIGURE 2. Mass distribution of finally-selected  $D^0 \rightarrow \pi^+ \pi^- \mu^+ \mu^-$  candidates in the dimuon-mass regions with fit projection overlaid [16].

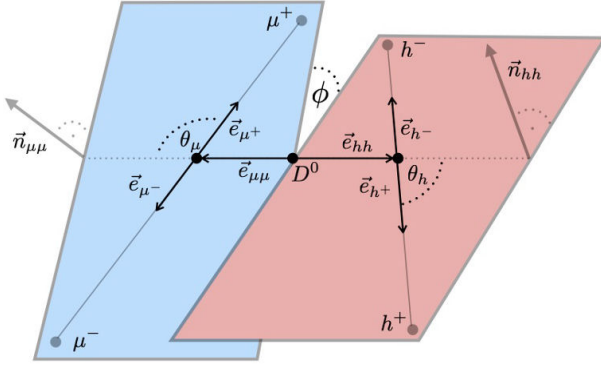


FIGURE 3. Diagram showing the definition of the three relevant angles for the  $D^0 \rightarrow h^+ h^- \mu^+ \mu^-$  asymmetries measurement: the angle  $\theta_\mu$  between the  $\mu^+$  ( $\mu^-$ ) direction and the direction opposite to the  $D^0$  ( $\bar{D}^0$ ) meson in the dimuon rest frame, the angle  $\theta_h$  between the  $h^+$  ( $h^-$ ) direction and the direction opposite to the  $D^0$  ( $\bar{D}^0$ ) meson in the dihadron rest frame, and the angle  $\phi$  between the two planes formed by the dimuon and the dihadron systems in the rest frame of the  $D^0$  meson [16].

ing fractions [11]. They can be suppressed by requiring PID criteria on the muons. Requirements on the MV classifier response and muon PID criteria are simultaneously optimized by maximising the figure of merit  $\epsilon_{h^+ h^- \mu^+ \mu^-} / (5/2 + \sqrt{N_{bkg}})$  [17], where  $\epsilon_{h^+ h^- \mu^+ \mu^-}$  is the total selection and reconstruction efficiency and  $N_{bkg}$  the expected background yield in the signal region.

The signal yields are measured by unbinned maximum likelihood fits to the  $D^0$  mass distributions. See Fig. 3 for the mass distributions of  $D^0 \rightarrow \pi^+ \pi^- \mu^+ \mu^-$  decays with fit projection overlaid in the considered dimuon-mass regions. The model used in the fit includes three components: signal, background from mis-identified hadronic background and combinatorial background.

BFs are measured in regions of dimuon mass where the statistical significance of the signal component exceeds three standard deviations with respect to the background-only hypothesis (low mass,  $\rho^0/\omega$  and  $\phi$  region). Otherwise, 90 % and 95 % C.L. upper limits are set. The branching fractions, integrated over dimuon mass, are measured to be:

$$\begin{aligned} \mathcal{B}(D^0 \rightarrow \pi^+ \pi^- \mu^+ \mu^-) &= (9.64 \pm 0.48 \pm 0.51 \pm 0.97) \times 10^{-7}, \\ \mathcal{B}(D^0 \rightarrow K^+ K^- \mu^+ \mu^-) &= (1.54 \pm 0.27 \pm 0.09 \pm 0.16) \times 10^{-7}, \end{aligned} \quad (1)$$

where the uncertainties are statistical, systematic and due to the limited knowledge of the normalisation mode branching fraction. These are the rarest charm meson decays ever observed. The measured branching fractions (or upper limits) in regions of dimuon mass for  $D^0 \rightarrow \pi^+ \pi^- \mu^+ \mu^-$  and  $D^0 \rightarrow K^+ K^- \mu^+ \mu^-$  decays are reported in Ref [16].

#### 4. Asymmetries in $D^0 \rightarrow h^+ h^- \mu^+ \mu^-$

The first measurement of angular and  $CP$  asymmetries in  $D^0 \rightarrow \pi^+ \pi^- \mu^+ \mu^-$  and  $D^0 \rightarrow K^+ K^- \mu^+ \mu^-$  decays is performed by the LHCb experiment using data collected in Run1 and part of Run2, corresponding to a total integrated luminosity of  $5 \text{ fb}^{-1}$  [18].

To fully describe the decay topology of these decays, five independent kinematic variables are defined: the masses of the dimuon and dihadron systems and three decay angles  $\theta_\mu$ ,  $\theta_h$  and  $\phi$  (see Fig. 4 for their definition). In addition to the  $CP$  asymmetry of the decay rate,  $A_{CP}$ , is defined as

$$A_{CP} = \frac{\Gamma(D^0 \rightarrow h^+ h^- \mu^+ \mu^-) - \Gamma(\bar{D}^0 \rightarrow h^+ h^- \mu^+ \mu^-)}{\Gamma(D^0 \rightarrow h^+ h^- \mu^+ \mu^-) + \Gamma(\bar{D}^0 \rightarrow h^+ h^- \mu^+ \mu^-)}. \quad (2)$$

LHCb has decided to study the following two angular observables: the forward-backward asymmetry in the dimuon system,  $A_{FB}$ , defined as

$$A_{FB} = \frac{\Gamma(\cos \theta_\mu > 0) - \Gamma(\cos \theta_\mu < 0)}{\Gamma(\cos \theta_\mu > 0) + \Gamma(\cos \theta_\mu < 0)}, \quad (3)$$

and the the triple-product asymmetry,  $A_{2\phi}$ , defined as

$$A_{2\phi} = \frac{\Gamma(\sin 2\phi > 0) - \Gamma(\sin 2\phi < 0)}{\Gamma(\sin 2\phi > 0) + \Gamma(\sin 2\phi < 0)}. \quad (4)$$

The candidate selection is similar to the analysis presented in the previous section. Fits to the  $D^0$ -mass distributions report signal yields of  $1326 \pm 45$  for  $D^0 \rightarrow \pi^+ \pi^- \mu^+ \mu^-$  and  $137 \pm 14$  for  $D^0 \rightarrow K^+ K^- \mu^+ \mu^-$  decays.

The signal candidates are further split into different tag categories defined by the flavour of  $D^0$  and  $\bar{D}^0$  mesons (to measure  $A_{CP}$ ) and the sign of  $\cos \theta_\mu$  and  $\sin 2\phi$  (to measure the angular asymmetries). Unbinned maximum-likelihood fits are performed to the  $D^0$  meson mass distributions to determine the signal asymmetries. All observables are measured both integrated and in regions of dimuon mass. The dimuon-mass integrated asymmetries are:

$$\begin{aligned} A_{FB}(D^0 \rightarrow \pi^+ \pi^- \mu^+ \mu^-) &= (3.3 \pm 3.7 \pm 0.6)\%, \\ A_{2\phi}(D^0 \rightarrow \pi^+ \pi^- \mu^+ \mu^-) &= (-0.6 \pm 3.7 \pm 0.6)\%, \\ A_{CP}(D^0 \rightarrow \pi^+ \pi^- \mu^+ \mu^-) &= (4.9 \pm 3.8 \pm 0.7)\%, \\ A_{FB}(D^0 \rightarrow K^+ K^- \mu^+ \mu^-) &= (0 \pm 11 \pm 2)\%, \\ A_{2\phi}(D^0 \rightarrow K^+ K^- \mu^+ \mu^-) &= (9 \pm 11 \pm 1)\%, \\ A_{CP}(D^0 \rightarrow K^+ K^- \mu^+ \mu^-) &= (0 \pm 11 \pm 2)\%, \end{aligned} \quad (5)$$

where the first uncertainty is statistical and the second systematic.

Results of the observables measured in regions of dimuon mass can be found in Ref [18]. All results are consistent with the SM predictions and will help to constrain the parameter space of NP models [19, 20].

TABLE I. Branching fractions limits and asymmetries uncertainties for various leptonic and semileptonic rare charm decays analysed by the LHCb collaboration. The table reports Run1-2 (2011-2018) already public measurements and extrapolations, based on the expected data collected, of limits and uncertainties for the two major upgrades. The current measurements presented are performed with different size of data from different years.

Mode	Current measurements		Upgrade1 (50 fb <sup>-1</sup> )	Upgrade2 (300 fb <sup>-1</sup> )
Branching fractions limits (away from resonances)				
$D^0 \rightarrow \mu^+ \mu^-$	$6.2 \times 10^{-9}$	[24]	$4.2 \times 10^{-10}$	$1.3 \times 10^{-10}$
$D^+ \rightarrow \pi^+ \mu^+ \mu^-$	$6.7 \times 10^{-8}$	[16]	$10^{-8}$	$3 \times 10^{-9}$
$D_{(s)}^+ \rightarrow K^+ \mu^+ \mu^-$	$2.6 \times 10^{-8}$	[16]	$10^{-8}$	$3 \times 10^{-9}$
$\Lambda_c^+ \rightarrow p \mu^+ \mu^-$	$7.7 \times 10^{-8}$	[25]	$1.1 \times 10^{-8}$	$4.4 \times 10^{-9}$
$D^0 \rightarrow e^\pm \mu^\mp$	$1.3 \times 10^{-8}$	[26]	$10^{-9}$	$4.1 \times 10^{-9}$
Asymmetries uncertainties				
$D^+ \rightarrow \pi^+ \mu^+ \mu^-$			0.2 %	0.08 %
$D^0 \rightarrow \pi^+ \pi^- \mu^+ \mu^-$	3.8 %	[18]	1 %	0.4 %
$D^0 \rightarrow K^- \pi^+ \mu^+ \mu^-$			0.3 %	0.13 %
$D^0 \rightarrow K^+ \pi^- \mu^+ \mu^-$			12 %	5 %
$D^0 \rightarrow K^+ K^- \mu^+ \mu^-$	11 %	[18]	4 %	1.7 %

## 5. Conclusion and prospects

The LHCb collaboration is investing lots of effort in the study of rare charm decays comprising charged leptons in the final state. The analyses discussed in these proceedings are performed using data collected by LHCb in Run1 and Run2 and show examples of the broad spectrum of measurements that can be performed in rare decays of neutral and charged  $D$  mesons at LHCb. This includes searches for rare and forbidden decays, as well as studies of  $CP$  and angular asymmetries in resonance-dominated decay modes.

The LHCb collaboration will continue exploiting its current and future data sets to expand even more the range of studies in rare charm. Currently, the LHCb detector is undergoing a first major upgrade with the aim to collect data corresponding to 50 fb<sup>-1</sup> by 2030 [21]. The instantaneous luminosity of the LHC is expected to increase by a factor five, reaching  $2 \times 10^{33}$  cm<sup>-2</sup> s<sup>-1</sup>. To cope with the increase in the interaction rate, the selection of events will be performed by a purely software based trigger system [22] and all sub-detectors have to be upgraded. A second major upgrade of

the LHCb detector is planned for 2030 in order to operate at a luminosity up to  $2 \times 10^{34}$  cm<sup>-2</sup> s<sup>-1</sup>, ten times more than the first upgrade. Intrinsic performance of the experiment will be improved with new detector components to be ready to collect 300 fb<sup>-1</sup> [23].

The first column in Table I reports current limits on branching fractions of benchmark in leptonic/semileptonic rare charm decays and sensitivities of measurements of angular and  $CP$  asymmetries. The extrapolations in the second and third column are based on the expected integrated luminosities after the detector upgrades discussed earlier. Improving the current results' precision will be crucial to constrain scenarios of physics beyond the SM.

## Acknowledgments

This work was supported by the European Research Council (ERC) under the European Union's Horizon 2020 research and innovation programme under grant agreement No 724777 "RECEPT".

1. S. L. Glashow, J. Iliopoulos and L. Maiani, Weak Interactions with Lepton-Hadron Symmetry, *Phys. Rev. D* **2** (1970) 1285, <https://doi.org/10.1103/PhysRevD.2.1285>.
2. L. Cappiello, O. Cata and G. D'Ambrosio, Standard Model prediction and new physics tests for  $D^0 \rightarrow h^+ h^- \ell^+ \ell^-$  ( $h = \pi, K; \ell = e, \mu$ ), *JHEP* **04** (2013) 135, [https://doi.org/10.1007/JHEP04\(2013\)135](https://doi.org/10.1007/JHEP04(2013)135).
3. S. De Boer and G. Hiller, Null tests from angular distributions in  $D \rightarrow P_1 P_2 l^+ l^-$ ,  $l = e, \mu$  decays on and off peak, *Phys.*

*Rev. D* **98** (2018) 035041, <https://doi.org/10.1103/PhysRevD.98.035041>.

4. S. Fajfer and S. Prelovsek, Effects of littlest Higgs model in rare D meson decays, *Phys. Rev. D* **73** (2006) 054026, <https://doi.org/10.1103/PhysRevD.73.054026>.
5. I. I. Bigi and A. Paul, On CP Asymmetries in Two-, Three- and Four-Body D Decays, *JHEP* **03** (2012) 021, [https://doi.org/10.1007/JHEP03\(2012\)021](https://doi.org/10.1007/JHEP03(2012)021).
6. A. Paul, A. De La Puente and I. I. Bigi, Manifestations of warped extra dimension in rare charm decays and asymmetries,



- Phys. Rev. D **90** (2014) 014035, <https://doi.org/10.1103/PhysRevD.90.014035>.
7. S. Fajfer and N. Košnik, Resonance catalyzed CP asymmetries in  $D^+ \ell^+ \ell^-$ , Phys. Rev. D **87** (2013) 054026, <https://doi.org/10.1103/PhysRevD.87.054026>.
  8. R. Aaij *et al.* [LHCb], LHCb Detector Performance, Int. J. Mod. Phys. A **30** (2015) 1530022, <https://doi.org/10.1142/S0217751X15300227>.
  9. A. A. Alves, Jr. *et al.* [LHCb], The LHCb Detector at the LHC, JINST **3** (2008) S08005, <https://doi.org/10.1088/1748-0221/3/08/S08005>.
  10. R. Aaij *et al.* [LHCb], Searches for 25 rare and forbidden decays of  $D^+$  and  $D_s^+$  mesons, JHEP **06** (2021) 044, [https://doi.org/10.1007/JHEP06\(2021\)044](https://doi.org/10.1007/JHEP06(2021)044).
  11. M. Tanabashi *et al.* [Particle Data Group], Review of Particle Physics, Phys. Rev. D **98** (2018) 030001, <https://doi.org/10.1103/PhysRevD.98.030001>.
  12. A. L. Read, Presentation of search results: The CLs technique, J. Phys. G **28** (2002) 2693, <https://doi.org/10.1088/0954-3899/28/10/313>.
  13. R. Aaij *et al.* [LHCb], Search for  $D_{(s)}^+ \rightarrow \pi^+ \mu^+ \mu^-$  and  $D_{(s)}^+ \rightarrow \pi^- \mu^+$  decays, Phys. Lett. B **724** (2013) 203, <https://doi.org/10.1016/j.physletb.2013.06.010>.
  14. J. P. Lees *et al.* [BaBar], Searches for Rare or Forbidden Semileptonic Charm Decays, Phys. Rev. D **84** (2011) 072006, <https://doi.org/10.1103/PhysRevD.84.072006>.
  15. P. Rubin *et al.* [CLEO], Search for rare and forbidden decays of charm and charmed-strange mesons to final states  $h^\pm e^\mp e^+$ , Phys. Rev. D **82** (2010) 092007, <https://doi.org/10.1103/PhysRevD.82.092007>.
  16. R. Aaij *et al.* [LHCb], Observation of  $D^0$  meson decays to  $\pi^+ \pi^- \mu^+ \mu^-$  and  $K^+ K^- \mu^+ \mu^-$  final states, Phys. Rev. Lett. **119** (2017) 181805, <https://doi.org/10.1103/PhysRevLett.119.181805>.
  17. G. Punzi, Sensitivity of searches for new signals and its optimization, eConf **C030908** (2003), MODT002, [arXiv:physics/0308063 [physics]].
  18. R. Aaij *et al.* [LHCb], Measurement of Angular and CP Asymmetries in  $D^0 \rightarrow \pi^+ \pi^- \mu^+ \mu^-$  and  $D^0 \rightarrow K^+ K^- \mu^+ \mu^-$  decays, Phys. Rev. Lett. **121** (2018) 091801, <https://doi.org/10.1103/PhysRevLett.121.091801>.
  19. S. Fajfer and N. Košnik, Prospects of discovering new physics in rare charm decays, Eur. Phys. J. C **75** (2015) 567, <https://doi.org/10.1140/epjc/s10052-015-3801-2>.
  20. S. de Boer and G. Hiller, Flavor and new physics opportunities with rare charm decays into leptons, Phys. Rev. D **93** (2016) 074001, <https://doi.org/10.1103/PhysRevD.93.074001>.
  21. R. Aaij *et al.* [LHCb], Letter of Intent for the LHCb Upgrade, CERN-LHCC-2011-001.
  22. J. Albrecht, C. Fitzpatrick, V. Gligorov and G. Raven, The upgrade of the LHCb trigger system, JINST **9** (2014) C10026, <https://doi.org/10.1088/1748-0221/9/10/C10026>.
  23. R. Aaij *et al.* [LHCb], Physics case for an LHCb Upgrade II - Opportunities in flavour physics, and beyond, in the HL-LHC era, [arXiv:1808.08865 [hep-ex]].
  24. R. Aaij *et al.* [LHCb], Search for the rare decay  $D^0 \rightarrow \mu^+ \mu^-$ , Phys. Lett. B **725** (2013) 15, <https://doi.org/10.1016/j.physletb.2013.06.037>.
  25. R. Aaij *et al.* [LHCb], Search for the rare decay  $\Lambda_c^+ \rightarrow p \mu^+ \mu^-$ , Phys. Rev. D **97** (2018) 091101, <https://doi.org/10.1103/PhysRevD.97.091101>.
  26. R. Aaij *et al.* [LHCb], Search for the lepton-flavour violating decay  $D^0 \rightarrow e^\pm \mu^\mp$ , Phys. Lett. B **754** (2016) 167, <https://doi.org/10.1016/j.physletb.2016.01.029>.